Original Article

The roles of lncRNA *AP001469.3* in clinical implications, immune landscape and carcinogenesis of colorectal cancer

Tao Chen[1,2]^, Qiusheng Jiang[2], Zhenlin Wang[1], Hongqiang Zhang[1], Zan Fu[1]^

[1]Department of General Surgery, the First Affiliated Hospital of Nanjing Medical University, Nanjing, China; [2]Department of General Surgery, Nanjing Pukou People's Hospital, Nanjing, China

Contributions: (I) Conception and design: Z Fu, T Chen; (II) Administrative support: Z Fu; (III) Provision of study materials or patients: Q Jiang, Z Wang, Z Fu; (IV) Collection and assembly of data: T Chen, H Zhang; (V) Data analysis and interpretation: T Chen, Z Fu; (VI) Manuscript writing: All authors; (VII) Final approval of manuscript: All authors.

Correspondence to: Zan Fu, PhD. Department of General Surgery, the First Affiliated Hospital of Nanjing Medical University, 300 Guangzhou Road, Gulou District, Nanjing 210029, China. Email: fuzan1971@njmu.edu.cn.

Background: Previously, long non-coding RNA (lncRNA) gene *AP001469.3* was reported to participate in the construction of an immune-related lncRNA signature, which showed promising clinical predictive value in colorectal cancer (CRC) patients. However, the clinical and immunological significance and biological function of *AP001469.3* in CRC remain unclear. In this study, we aim to explore the roles of *AP001469.3* in CRC progression, thereby opening an avenue for CRC treatment.

Methods: Our study collected data from The Cancer Genome Atlas (TCGA) database and investigated the role of *AP001469.3* in CRC through bioinformatics analysis. Cell-type Identification By Estimating Relative Subsets Of known RNA Transcripts (CIBERSORT) and Estimation of STromal and Immune cells in MAlignant Tumor tissues using Expression data (ESTIMATE) methods evaluated the immune infiltration. The biological functions of *AP001469.3* in CRC were validated by *in vitro* experiments. Gene set enrichment analysis (GSEA) was used to estimate the enrichment of functional pathways and gene signatures.

Results: In this work, high expression of *AP001469.3* was found in CRC and was positively associated with tumor-node-metastasis (TNM) stage in CRC. *AP001469.3* expression had a strong relationship with microsatellite instability (MSI) in colon adenocarcinoma (COAD). Additionally, *AP001469.3* expression was associated with StromalScore, ImmuneScore, ESTIMATEScore, immune cell infiltration (ICI) levels and immune checkpoint (ICP) genes expression in CRC. Subsequent results showed that immunotherapy could be more effective in CRC patients with low-*AP001469.3* expression using the immunophenoscore (IPS). We confirmed that the transcript of *AP001469.3* gene *ENST00000430259* was highly expressed in CRC tissues and cell lines. *In vitro* experiments indicated that *ENST00000430259* knockdown reduced the proliferation, migration and invasion of CRC cells. Finally, our GSEA results showed that the majority of the differentially enriched signaling pathways between the high- and low-*AP001469.3* expression groups were immune-related.

Conclusions: Taken together, our study demonstrates that lncRNA gene *AP001469.3* is associated with immunological characteristics in CRC and promotes malignant progression of CRC. Moreover, *AP001469.3* can be potentially used as an immunotherapeutic indicator and a therapeutic target for CRC patients.

Keywords: Long non-coding RNA (lncRNA); *AP001469.3*; colorectal cancer (CRC); immune microenvironment; immunotherapy

Submitted Jan 20, 2024. Accepted for publication Jun 02, 2024. Published online Jul 19, 2024.
doi: 10.21037/tcr-24-145
View this article at: https://dx.doi.org/10.21037/tcr-24-145

^ ORCID: Tao Chen, 0000-0001-8071-4959; Zan Fu, 0000-0003-4753-1821.

Introduction

Colorectal cancer (CRC) is an aggressive malignant tumor of the digestive system. It has become the second leading cause of cancer-related mortality worldwide (1). Due to the lack of significant clinical symptoms in the early stages, most of CRC patients already have advanced or metastatic lesions when diagnosed (2). At present, traditional treatments such as surgery and chemotherapy have achieved certain efficacy, but the treatment effect is not satisfactory, and problems such as recurrence and metastasis of the disease still exist (3). Immunotherapy has become a hot research topic in the field of CRC treatment (4). Specifically, it includes restoring the mechanism by which tumor cells evade the immune system and enhancing the anti-tumor immune response. Current CRC immunotherapy research focuses on anti-cytotoxic T-lymphocyte-associated antigen-4 (CTLA-4) antibodies, anti-programmed cell death protein-1 (PD-1)/programmed cell death protein-ligand 1 (PD-L1) antibodies, and chimeric antigen receptor T (CAR-T) cell therapy (4). However, relying on single immunotherapy alone is often difficult to clear tumors comprehensively and effectively, which is one of the current challenges in the immunotherapy field (5). Therefore, more investigations are desperately needed to provide potential targets for treatment of advanced CRC patients.

Long non-coding RNAs (lncRNAs), defined as transcripts longer than 200 nucleotides with little protein-coding potential, constitute a large proportion of the transcriptome (6). Mutations and misregulation of lncRNAs appear to play vital roles in various biological processes associated with tumorigenesis, tumor invasion and tumor metastasis (7). Researches have shown that lncRNAs can also influence cancer's malignant progression by regulating the tumor immune microenvironment (TIME), such as the immune cell infiltration (ICI) and the expression of immune checkpoint (ICP) genes (8-10). Mounting evidence suggests that the TIME serves pivotal roles in determining tumor progression and immunotherapy response in CRC (11,12). Previously, lncRNA gene *AP001469.3* was reported in one bioinformatics study to participate in the construction of immune-related lncRNA pair signature, which showed promising clinical predictive value for CRC patients (13). However, the role of *AP001469.3* in clinical implications, immune landscape and carcinogenesis of CRC was unexplored.

Our study sought to confirm the expression of *AP001469.3* in pan-cancer and its associations with prognosis and clinical characteristics of CRC patients using the transcriptome data from The Cancer Genome Atlas (TCGA) database. Additionally, the correlation of *AP001469.3* expression with TIME was explored in CRC using bioinformatics tools and algorithms. Further *in vitro* studies indicated that *AP001469.3* functioned as an oncogene to promote the malignant progression of CRC, and the potential molecular functional mechanism of *AP001469.3* in CRC was also explored using gene set enrichment analysis (GSEA). We present this article in accordance with the MDAR reporting checklist (available at https://tcr.amegroups.com/article/view/10.21037/tcr-24-145/rc).

Highlight box

Key findings

- Long non-coding RNA (lncRNA) gene *AP001469.3* was significantly associated with immunological characteristics in colorectal cancer (CRC) and promoted malignant progression of CRC *in vitro*.

What is known and what is new?

- Previous study reported that *AP001469.3* could participate in the construction of an immune-related lncRNA prognostic signature in CRC. However, the clinical and immunological significance and biological function of *AP001469.3* in CRC remain unclear.
- In this study, the role of *AP001469.3* in clinical implications, immune landscape and carcinogenesis of CRC was first explored in oncology research.

What is the implication, and what should change now?

- LncRNA *AP001469.3* can be potentially used as an immunotherapeutic indicator and a therapeutic target for CRC patients.

Methods

Retrieval and processing of TCGA pan-cancer dataset and TCGA-CRC dataset

The TCGA pan-cancer dataset with RNA-sequencing (RNA-seq) data [fragments per kilobase million (FPKM)] and clinical data was downloaded from University of California Santa Cruz (UCSC) Xena Data Browser (https://xenabrowser.net/datapages/) (14). The TCGA pan-cancer dataset included 11,057 samples and 60,484 genes. The RNA-seq data of *ENSG00000239415* (*AP001469.3*) was extracted and $\log_2$(FPKM+1) transformation was performed.

The updated TCGA colon adenocarcinoma (TCGA-

COAD) dataset and TCGA rectum adenocarcinoma (TCGA-READ) dataset with RNA-seq data [transcript per million (TPM)] and clinical data were downloaded from Genomic Data Commons (GDC) Data Portal (https://portal.gdc.cancer.gov/). Subsequently, TCGA-COAD and TCGA-READ were combined into a TCGA-CRC dataset for subsequent analysis. After deleting the cases with insufficient or missing data, we obtained the transcriptome data of 618 CRC tissue specimens and 51 normal tissue specimens. The RNA-seq data of *ENSG00000239415* (*AP001469.3*) was extracted and $\log_2$(TPM+1) transformation was performed.

Survival analysis

Patients were classified into high- and low-*AP001469.3* expression groups and the cut-off was the median of *AP001469.3* expression according to the data downloaded from TCGA. Thereafter, Kaplan-Meier (KM) method was used to compare overall survival (OS), disease-specific survival (DSS) and disease-free interval (DFI) in two groups of patients using the survival R package. The survminer R package was applied to determine the optimal cut-off value of *AP001469.3* expression in classifying CRC samples of TCGA-CRC dataset into high- and low-*AP001469.3* expression groups. The difference between curves was examined using the log-rank test, and a value of $P<0.05$ was considered significant.

Immunological characteristics analysis

Tumor mutation burden (TMB) and microsatellite instability (MSI) data were obtained from the TCGA database. The correlations between *AP001469.3* expression and TMB and MSI were analyzed by Spearman correlation analysis, and radar plots using the fmsb R package were displayed as final results. The Estimation of STromal and Immune cells in MAlignant Tumor tissues using Expression data (ESTIMATE) algorithm estimated stromal fractions and immune fractions in tumor tissues with data downloaded from the public website (https://sourceforge.net/projects/estimateproject/). Based on the RNA-seq data of CRC samples from the TCGA database, the ESTIMATE method was applied to calculate the values of each sample's overall stroma level (StromalScore), immunocyte infiltration (ImmuneScore), and combination (ESTIMATEScore) (15). Based on the 1,000 permutations of leukocyte signature matrix (LM22) signature, the Cell-type Identification By Estimating Relative Subsets Of known RNA Transcripts (CIBERSORT) method was employed to estimate the infiltrating percentages of 22 different types of immune cells in the CRC TIME (16). The correlation between *AP001469.3* expression and ICI was analyzed by Spearman correlation analysis. In addition, 47 ICP genes were obtained from previous research (17). The correlation between *AP001469.3* expression and ICP genes was examined by Pearson correlation analysis. Finally, the immunophenoscore (IPS) of CRC patients in TCGA was acquired from The Cancer Immunome Atlas (TCIA) database (https://tcia.at/).

GSEA

Kyoto Encyclopedia of Genes and Genomes (KEGG) and Gene Ontology (GO) pathways were downloaded from Molecular Signatures Database (MSigDB) (18). After separating CRC patients into high- and low-*AP001469.3* expression groups, we explored the KEGG and the GO pathways of *AP001469.3* by using GSEA with the clusterProfiler and ggplot2 R packages. The expression level of *AP001469.3* was used as a phenotype label.

Patients sample collection

This study was supported by the Ethics Committee of the First Affiliated Hospital of Nanjing Medical University, China, and all the included patients volunteered to participate. The CRC specimens and adjacent normal tissues were obtained from ten patients who underwent surgery from November 2023 to December 2023. The study was conducted in accordance with the Declaration of Helsinki (as revised in 2013). The study was approved by the Ethics Committee of the First Affiliated Hospital of Nanjing Medical University, China (No. 2023-SR-206) and informed consent was obtained from all individual participants.

Cell culture and transfection

The human CRC cell lines HCT116, SW620, SW480, and DLD-1 and the human normal intestinal epithelial cell line FHC were purchased from the Chinese Academy of Sciences (Shanghai, China). FHC, DLD-1 and SW620 cell lines were cultured in Roswell Park Memorial Institute (RPMI)-1640 medium (HyClone, Logan, UT, USA). HCT116 and SW480 cell lines were cultured in Dulbecco's Modified

Eagle's Medium (DMEM) (HyClone, Logan, UT, USA). All media were supplemented with 10% fetal bovine serum (FBS), 100 U/mL penicillin and 100 mg/mL streptomycin. All cells were cultured at 37 ℃ in a humid incubator with 5% CO_2. The small interfering RNA (siRNA)-*ENST00000430259* and negative control (si-NC) were synthesized from GeneChem (Shanghai, China), which were transfected into CRC cells using Lipofectamine 3000 (Invitrogen, Carlsbad, USA) according to the manufacturer's protocols. The sequences of siRNA were as follow: si-*ENST00000430259*, 5'-GAGUUGAUUGUUAUUUCAAGC-3' (sense) and 5'-UUGAAAUAACAAUCAACUCUU-3' (antisense); si-NC, 5'-UUCUCCGAACGUGUCACGUTT-3' (sense) and 5'-ACGUGACACGUUCGGAGAATT-3' (antisense).

Quantitative real-time polymerase chain reaction (qRT-PCR)

Total RNA was extracted using TRIzol reagent (Invitrogen). Reverse transcriptase was used to convert the extracted total RNA into the complementary DNA (cDNA) template for qRT-PCR. Then qRT-PCR was conducted on an ABI PRISM 7900HT Sequence Detection System (Applied Biosystems, Foster City, CA, USA) using the corresponding PCR reagent according to the manufacturer's instructions. The primers used were as follows: *ENST00000430259*, 5'-ACTTGGCAACAGTCTTAGACCA-3' (forward) and 5'-AATGCCAAAAGTTTCTTTAAGGGG-3' (reverse); *ENST00000447037*, 5'-AGTAAGATGTGGTATTTGTGGACCT-3' (forward) and 5'-AAGCGTCTGAATCCCACCAG-3' (reverse); *β-actin*, 5'-GTGGACATCCGCAAAGAC-3' (forward) and 5'-AAAGGGTGTAACGCAACTA-3' (reverse). Relative expression was normalized to *β-actin* and calculated using the $2^{-\Delta\Delta CT}$ method.

Cell counting kit-8 (CCK-8) assays

CRC cells (1×10^4 cells/well) were seeded into 96-well plates and cultured in a 5% CO_2 cell incubator at 37 ℃ for 96 hours. 10 μL CCK-8 solution (Beyotime, Shanghai, China) was added to each plate at various time points (12, 24, 48, 72 and 96 hours) and cells were incubated for 2 hours at 37 ℃. The absorbance at 450 nm was measured by a microplate reader.

Transwell assays

Transwell assays were implemented to assess cell migration and invasion. 24-well Millicell hanging cell culture inserts (8.0 μm, Millipore, Bedford, MA, USA) were used as per manufacturer's protocol. For the migration assay, the bottom of the insert was seeded with 4×10^4 cells (per well) in 200 μL of serum-free medium, and then, 500 μL of medium containing 10% FBS was added to the lower chamber. To perform the invasion assays, Matrigel (BD Biosciences, Franklin Lakes, NJ, USA) was added to the insert, and then, 8×10^4 cells (per well) in serum-free medium were added to the upper chamber. Then, 500 μL complete medium with 10% FBS in the lower chamber served as a chemoattractant. After 24 hours of incubation, the cells on the bottom of the membrane were fixed and stained with 0.5% crystal violet for counting. We used light microscopy to observe the migrating and invading cells and randomly selected three fields for counting.

Wound healing assays

CRC cells (3×10^5 cells/well) were seeded into 6-well plates and cultured until the cell density reached 90%. Each well was scratched with a 10 μL pipette tip. Then, the cells were washed and incubated in an incubator at 37 ℃, and images of the same area of the wounds were captured at 0 and 24 hours. Finally, the wound area was analyzed by ImageJ.

Statistical analysis

All experiments were performed at least three times. All the data were analyzed and organized using R software (version 4.3.1) and GraphPad Prism 8.0 (GraphPad Software, CA, USA). The *t*-test was conducted to compare the differences between the two groups of data that conformed to the Gaussian distribution. The Wilcoxon test was used for the data that conformed to the non-Gaussian distribution. One-way analysis of variance (ANOVA) was conducted to compare multiple groups, and the Chi-squared test was conducted for categorical variables. All the data were presented as the mean ± standard deviation (SD) and $P<0.05$ was determined as statistically significant.

Results

AP001469.3 expression is upregulated and positively associated with tumor-node-metastasis (TNM) stage in CRC

To investigate the possible role of *AP001469.3* in carcinogenesis, we first assessed the expression level of the *AP001469.3* gene in 33 human cancers using the TCGA pan-cancer dataset

(*Figure 1A*). We found that *AP001469.3* was significantly upregulated in the tissues of colon adenocarcinoma (COAD) (P<0.001) and rectum adenocarcinoma (READ) (P<0.001) compared with their respective normal tissues. Additionally, *AP001469.3* was also found to be remarkably upregulated in eleven types of tumors compared with the respective control tissues, including bladder urothelial carcinoma (BLCA) (P<0.001), cholangiocarcinoma (CHOL) (P<0.001), esophageal carcinoma (ESCA) (P=0.002), glioblastoma multiforme (GBM) (P=0.01), head and neck squamous cell carcinoma (HNSC) (P<0.001), liver hepatocellular carcinoma (LIHC) (P<0.001), lung adenocarcinoma (LUAD) (P<0.001), lung squamous cell carcinoma (LUSC) (P<0.001), pheochromocytoma and paraganglioma (PCPG) (P=0.008), prostate adenocarcinoma (PRAD) (P<0.001) and stomach adenocarcinoma (STAD) (P<0.001). By contrast, *AP001469.3* was significantly downregulated in the tissues of kidney chromophobe (KICH) (P<0.001), kidney renal clear cell carcinoma (KIRC) (P<0.001) and thyroid carcinoma (THCA) (P=0.004) compared with the respective normal tissues.

After deleting the cases with insufficient or missing data, the clinical characteristics of 615 CRC patients from the TCGA-CRC dataset are displayed in *Table 1*. The prognostic value of *AP001469.3* on OS of CRC patients was evaluated using KM plotter. However, there was no significant difference in OS between the high and low expression groups of the *AP001469.3* gene when the cut-off was taken as the median value of *AP001469.3* expression (P=0.12, *Figure 1B*). But interestingly, when CRC samples were then classified into high- and low-*AP001469.3* expression groups with the optimal cut-off value of *AP001469.3* expression [$\log_2$(TPM+1)] at 2.08, which was determined using the survminer package, the survival analysis results showed that CRC patients with higher *AP001469.3* expression had significantly shorter OS time than those with lower *AP001469.3* expression (P=0.01, *Figure 1C*). Using KM plotter, we also evaluated the prognostic value of *AP001469.3* on OS (Figure S1), DSS (Figure S2) and DFI (Figure S3) of pan-cancer. Next, we analyzed the relationship between the expression level of *AP001469.3* and the clinical characteristics of CRC patients. The results showed that the expression of *AP001469.3* was increased along with the progression of metastasis (M) stage (P=0.002) and TNM stage (stage IV versus stage I, P=0.02; stage IV versus stage II, P=0.008; stage IV versus stage III, P=0.03) in CRC (*Figure 1D-1F*). Moreover, we also investigated the relationship between the expression of *AP001469.3* and TNM stage of pan-cancer (Figure S4). From the above results, we speculated that dysregulated *AP001469.3* expression might play a crucial part in the progression of CRC.

The correlations between AP001469.3 expression and TMB, MSI and ICP genes expression in pan-cancer

Previously, Sun *et al.* (13) screened the immune-related lncRNA gene *AP001469.3* using the Immport database

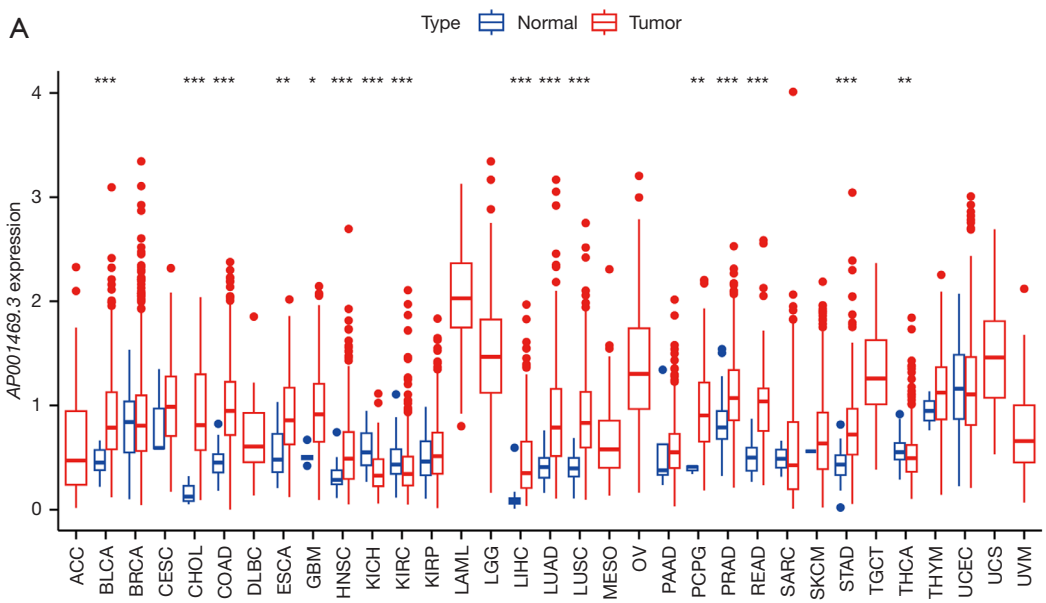

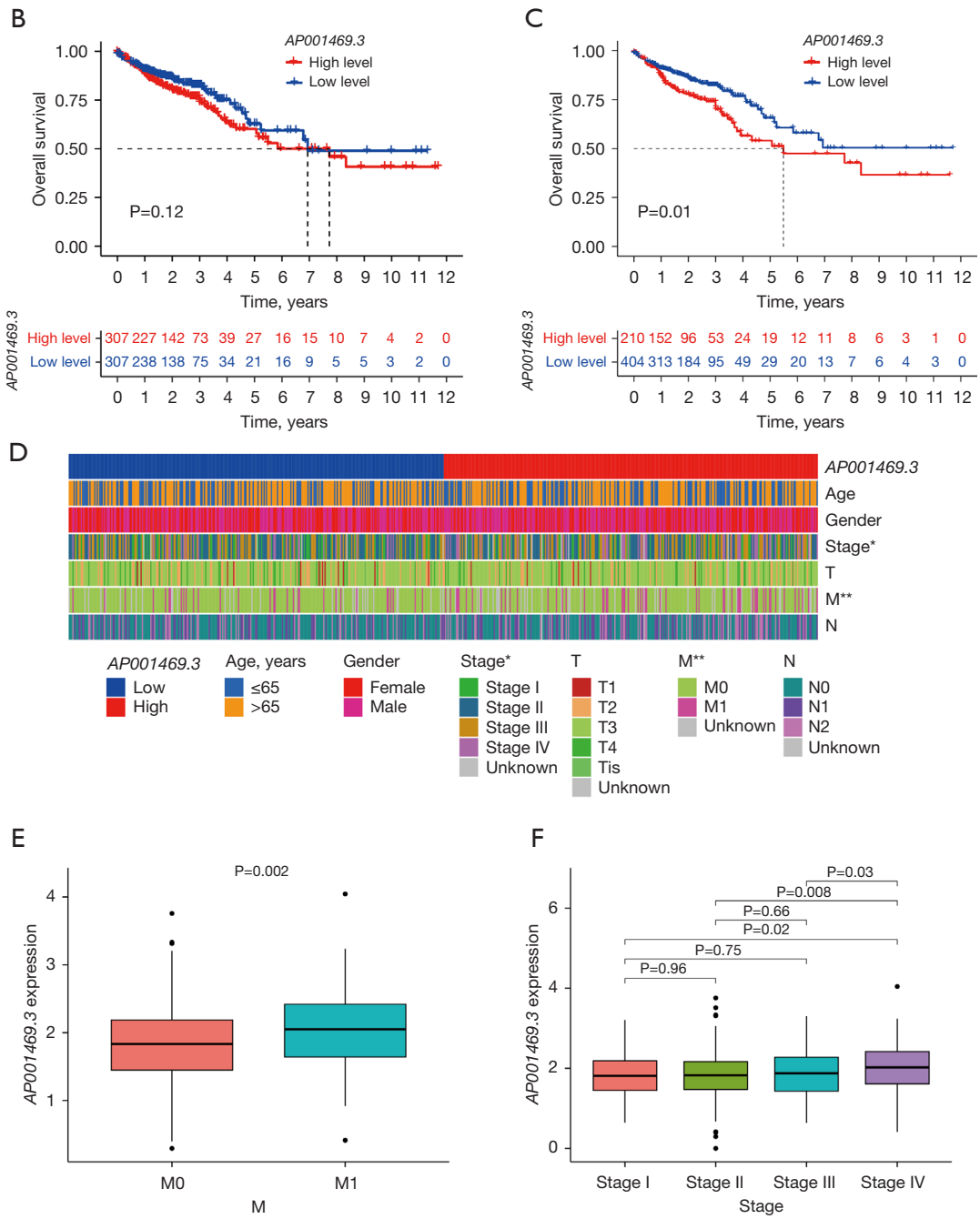

Figure 1 *AP001469.3* expression is upregulated and positively associated with TNM stage in CRC. (A) The expression level of *AP001469.3* in 33 human cancers from TCGA database. (B,C) KM method was used to compare OS between the high- and low-*AP001469.3* expression groups of CRC patients. The population was divided into the two groups according to the median expression level of *AP001469.3* (B) or the optimal cut-off value of *AP001469.3* expression [$\log_2$(TPM+1) =2.08] (C). The difference between curves was examined using the log-rank test. (D) The heatmap showed the relationship between *AP001469.3* expression and clinical characteristics of CRC patients. The data were derived from TCGA. Chi-squared test was conducted. (E,F) *AP001469.3* expression was increased along with the progression of M stage (E) and TNM stage (F) in CRC patients. The data were derived from TCGA. Wilcoxon test was conducted between two groups. *, P<0.05; **, P<0.01; ***, P<0.001. TNM, tumor-node-metastasis; CRC, colorectal cancer; TCGA, The Cancer Genome Atlas; KM, Kaplan-Meier; OS, overall survival; TPM, transcript per million.

Table 1 Baseline characteristics of TCGA-CRC patients included in clinical pathological analysis

Characteristic	Number of patients	Percentage
Age (years)		
≤65	264	42.9%
>65	351	57.1%
Gender		
Female	288	46.8%
Male	327	53.2%
Overall survival information		
Known	614	99.8%
Unknown	1	0.2%
Stage		
I	103	16.7%
II	228	37.1%
III	177	28.8%
IV	87	14.1%
Unknown	20	3.3%
T classification		
T1	19	3.1%
T2	104	16.9%
T3	421	68.4%
T4	69	11.2%
Tis	1	0.2%
Unknown	1	0.2%
N classification		
N0	349	56.7%
N1	147	23.9%
N2	116	18.9%
Unknown	3	0.5%
M classification		
M0	456	74.1%
M1	86	14.0%
Unknown	73	11.9%

TCGA, The Cancer Genome Atlas; CRC, colorectal cancer; T, tumor; N, node; M, metastasis.

(https://www.immport.org) and the co-expression analysis. As known, TMB and MSI are related to antitumor immunity and can predict the immunotherapy response in CRC patients (19,20). To investigate the role of *AP001469.3* in regulating the immune mechanism and immune response of the TIME, we analyzed the correlations between TMB and MSI and *AP001469.3* expression across 33 tumors of TCGA (*Figure 2A*,*2B*). The results showed that *AP001469.3* was significantly correlated with TMB and MSI in many kinds of cancers (all P<0.05). However, there was no significant correlation between *AP001469.3* expression and TMB in COAD (P=0.14) and READ (P=0.10). But interestingly, we found that *AP001469.3* expression was significantly negatively correlated with MSI in COAD (P<0.001).

Researches have proven that ICP genes, such as PD-1and its ligand PD-L1, can modulate the signaling pathways in regulating immune response and have an important role in the field of anti-cancer immunotherapy (21). Therefore, from a previous study (17), we obtained 47 ICP genes and assessed the correlation between the expression of *AP001469.3* and these ICP genes expression in pan-cancer. Pearson correlation coefficients were calculated to be differentially present in different cancer types. As shown in *Figure 2C*, *AP001469.3* expression was significantly correlated with more than 30 ICP genes in several cancers, such as COAD and GBM (all P<0.05). The above results indicated that *AP001469.3* might influence antitumor immunity by modifying the TIME in cancers.

AP001469.3 expression correlates with ICI levels and ICP genes expression in CRC

In order to further analyze the relationship between *AP001469.3* expression and the TIME in CRC, we calculated the StromalScore, ImmuneScore, and ESTIMATEScore of the high- and low-*AP001469.3* expression groups using the ESTIMATE method. The results showed that the low-*AP001469.3* expression group had a remarkably higher StromalScore (P<0.001), ImmuneScore (P<0.001) and ESTIMATEScore (P<0.001) compared with the high-*AP001469.3* expression group (*Figure 3A*), indicating that the immune and matrix components between the two groups were significantly

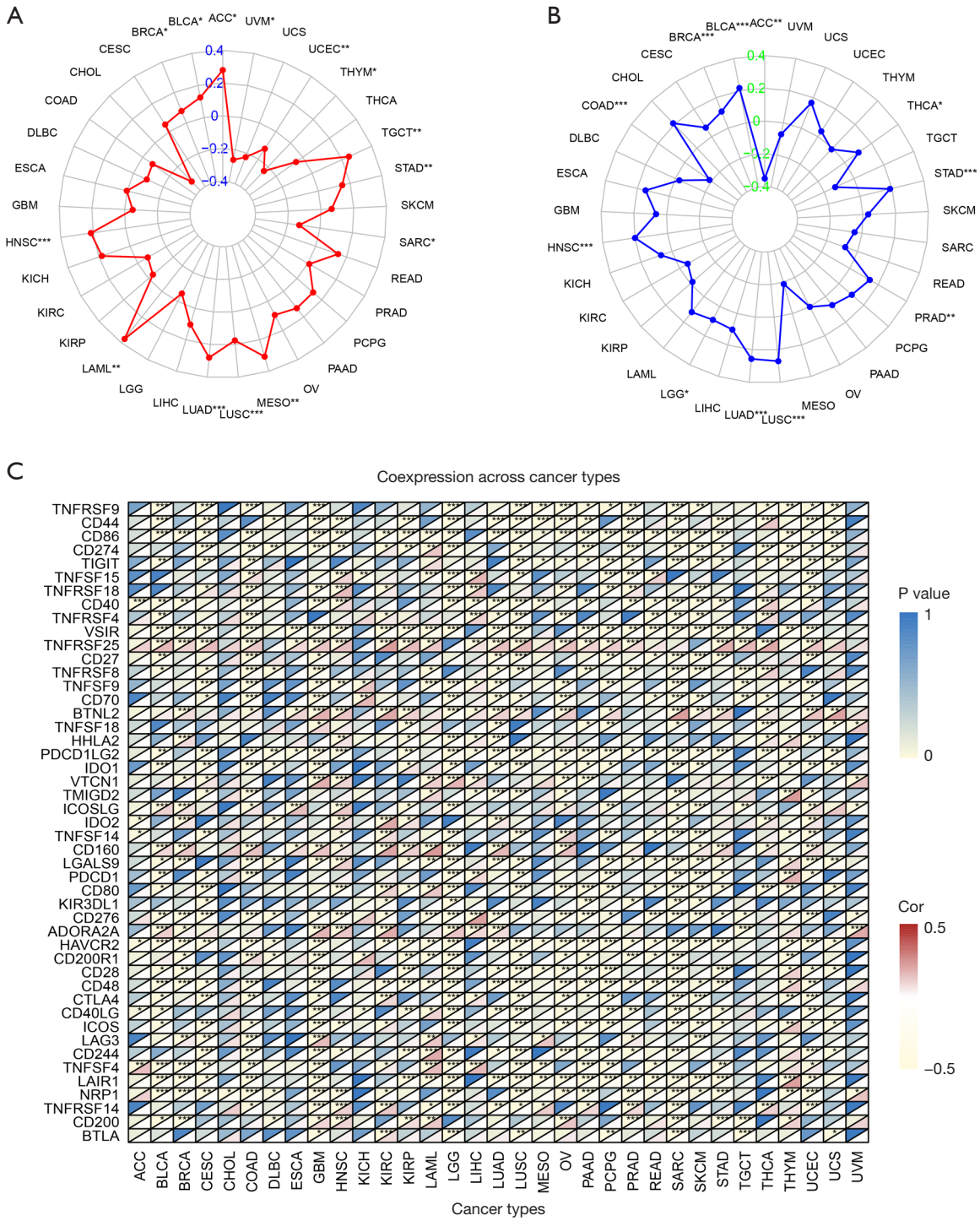

Figure 2 The correlations between *AP001469.3* expression and TMB, MSI and ICP genes expression in pan-cancer. (A,B) Spearman correlation analysis between TMB (A) and MSI (B) and *AP001469.3* expression across all tumors of TCGA. (C) Pearson correlation analysis between *AP001469.3* expression and ICP genes expression across all tumors of TCGA. *, P<0.05; **, P<0.01; ***, P<0.001. TMB, tumor mutational burden; MSI, microsatellite instability; ICP, immune checkpoint; TCGA, The Cancer Genome Atlas; Cor, correlation coefficients.

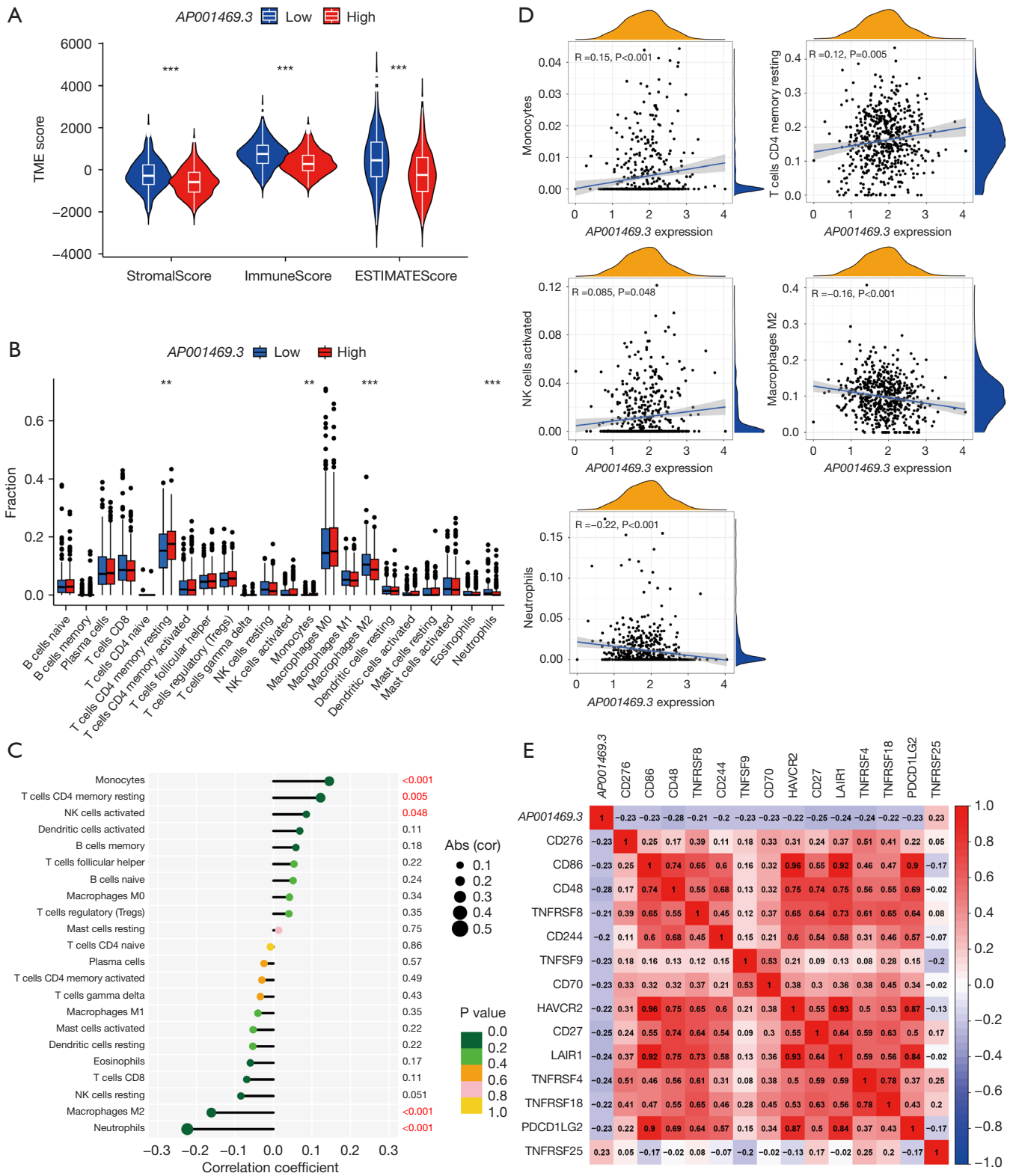

Figure 3 *AP001469.3* expression correlates with ICI levels and ICP genes expression in CRC. (A) The StromalScore, ImmuneScore, and ESTIMATEScore of the two groups with high and low expression of *AP001469.3* were calculated using the ESTIMATE method. (B) The

infiltrating percentages of 22 different types of immune cells between the two groups with high and low expression of *AP001469.3* were estimated by the CIBERSORT method. (C,D) Spearman correlation analysis between *AP001469.3* expression and 22 tumor-infiltrating immune cells was conducted (C), the results showed that the infiltration levels of monocytes, resting memory CD4 T cells, activated NK cells, M2 macrophages and neutrophils were significantly correlated with *AP001469.3* expression (D). (E) The correlation between *AP001469.3* expression and ICP genes was analyzed using Pearson correlation analysis, with an absolute value of correlation coefficient greater than 0.2. Wilcoxon test was conducted between two groups. **, P<0.01; ***, P<0.001. ICI, immune cell infiltration; ICP, immune checkpoint; CRC, colorectal cancer; ESTIMATE, Estimation of STromal and Immune cells in MAlignant Tumor tissues using Expression data; CIBERSORT, Cell-type Identification By Estimating Relative Subsets Of known RNA Transcripts; NK, natural killer; TME, tumor microenvironment; Abs (cor), absolute correlation coefficients.

different. Next, to explore the ability of *AP001469.3* to predict the ICI levels in the immune microenvironment of CRC, the CIBERSORT method was performed to determine the infiltrating percentages of 22 different types of immune cells. Our results suggested that four out of 22 immune cells were differentially enriched in high- and low-*AP001469.3* expression groups (all P<0.01, *Figure 3B*). We also performed the correlation analysis and found that the infiltration levels of monocytes (R=0.15, P<0.001), resting memory CD4 T cells (R=0.12, P=0.005) and activated natural killer (NK) cells (R=0.085, P=0.048) were significantly and positively correlated with *AP001469.3* expression, while the infiltration levels of M2 macrophages (R=–0.16, P<0.001) and neutrophils (R=–0.22, P<0.001) were significantly and negatively correlated with *AP001469.3* expression (*Figure 3C*,*3D*).

Furthermore, the correlation between *AP001469.3* expression and ICP genes was also analyzed in CRC. As shown in *Figure 3E* with an absolute value of correlation coefficient greater than 0.2, the majority of the ICP genes including CD276, CD86, CD48, TNFRSF8, CD244, TNFSF9, CD70, HAVCR2, CD27, LAIR1, TNFRSF4, TNFRSF18 and PDCD1LG2 were significantly and negatively correlated with *AP001469.3* expression (all P<0.001), while only TNFRSF25 was significantly and positively correlated with *AP001469.3* expression (P<0.001). Altogether, the above results indicated that *AP001469.3* might play an important role in regulating the immune response in the TIME of CRC by influencing ICI and ICP molecules.

The role of AP001469.3 expression in the prediction of immunotherapy response in CRC

Based on the differential immune infiltration between high- and low-*AP001469.3* expression groups in CRC, we suspected a difference in response to immunotherapy between the two groups. As known, TCIA is a database based on TCGA and provides comprehensive immunogenomic analysis (https://tcia.at/). IPS primarily includes four components (effector cells, immunosuppressive cells, major histocompatibility complex molecules, and immune modulators) that determine tumor immunogenicity (22). The IPS is calculated on a 0–10 scale, and higher IPS is associated with increased immunogenicity. Consequently, a higher IPS for a patient indicates that the patient can benefit from immunotherapy (22). Here we obtained the IPS scores of CRC patients from TCIA database. Then we divided the CRC patients into four subgroups according to their usage of anti-PD-1 and anti-CTLA-4 immunotherapies: CTLA-4 negative PD-1 negative (*Figure 4A*), CTLA-4 negative PD-1 positive (*Figure 4B*), CTLA-4 positive PD-1 negative (*Figure 4C*), and CTLA-4 positive PD-1 positive (*Figure 4D*). Notably, our results pointed out that in subgroups of CTLA-4 negative PD-1 positive (P=0.03) and CTLA-4 positive PD-1 positive (P<0.001), the IPS scores of low-*AP001469.3* expression group were higher than those of high-*AP001469.3* expression group. On the contrary, in subgroups of CTLA-4 negative PD-1 negative (P=0.33) and CTLA-4 positive PD-1 negative (P=0.84), there was no significant difference in IPS scores between the high and low expression groups of the *AP001469.3* gene. The above results indicated that CRC patients with low-*AP001469.3* expression might benefit more from immunotherapy based on anti-PD-1 rather than anti-CTLA-4.

The transcript of AP001469.3 gene ENST00000430259 is overexpressed in CRC tissues and cell lines

In our study, we confirmed that *AP001469.3* gene has two transcripts *ENST00000447037* (686bp) and *ENST00000430259* (2,014bp) through the Ensembl database (https://asia.ensembl.org/index.html) (23). Using

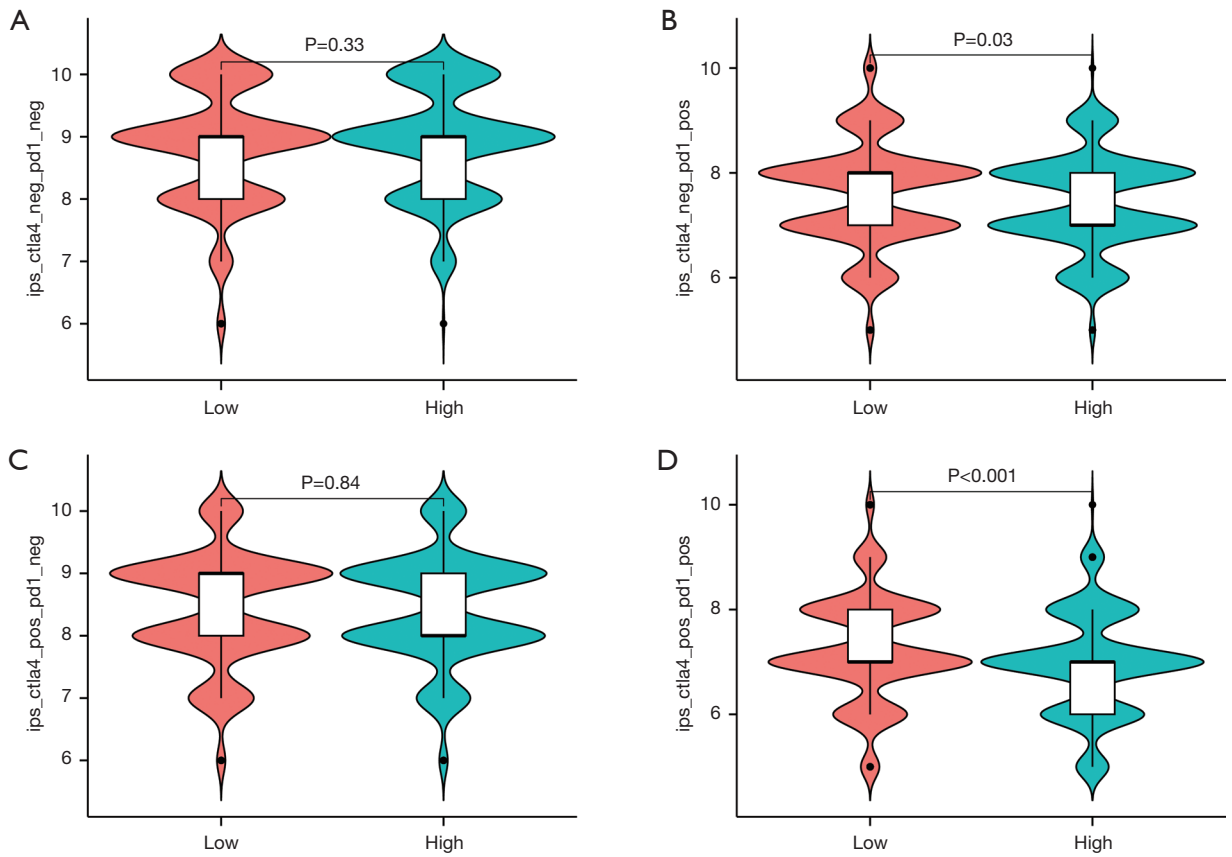

Figure 4 The role of *AP001469.3* expression in the prediction of immunotherapy response in CRC. (A-D) Correlation of IPS with *AP001469.3* expression was analyzed among four subgroups including CTLA-4 negative PD-1 negative (A), CTLA-4 negative PD-1 positive (B), CTLA-4 positive PD-1 negative (C), and CTLA-4 positive PD-1 positive (D). Wilcoxon test was conducted between two groups. CRC, colorectal cancer; IPS, Immunophenoscore; CTLA-4, cytotoxic T-lymphocyte-associated antigen-4; PD-1, programmed cell death protein-1.

qRT-PCR we found that in three cases of CRC tissues, the expression level of transcript *ENST00000430259* was much higher than that of transcript *ENST00000447037* (P=0.006, *Figure 5A*), indicating that *ENST00000430259* might play a leading role in the biological function of *AP001469.3* gene. Consequently, *ENST00000430259* was selected as the research target in the subsequent experiments due to its relatively high abundance. Using qRT-PCR, our results showed that *ENST00000430259* was aberrantly overexpressed in ten cases of CRC tissues when compared with their respective controls (P<0.001, *Figure 5B*). Consistently, *ENST00000430259* expression was verified to be significantly higher in CRC cell lines (HCT116, SW620, SW480 and DLD-1) than in the normal intestinal epithelial cell line FHC using qRT-PCR (all P<0.05, *Figure 5C*).

ENST00000430259 functions as an oncogenic lncRNA in vitro in CRC

To determine the potential function of *ENST00000430259* in CRC, we first knocked down *ENST00000430259* expression in DLD-1 cells and verified its efficiency by qRT-PCR (P<0.001, *Figure 6A*). CCK-8 assays revealed that *ENST00000430259* knockdown suppressed the proliferation of DLD-1 cells (P<0.001, *Figure 6B*). Additionally, transwell assays revealed that *ENST00000430259* knockdown reduced the migration and invasion abilities of DLD-1 cells (P<0.001, *Figure 6C*). Furthermore, wound healing assays also showed that *ENST00000430259* knockdown reduced the migration abilities of DLD-1 cells (P<0.001, *Figure 6D*). Thus, the results of *in vitro* experiments demonstrated that the transcript of *AP001469.3* gene *ENST00000430259* functioned as an oncogenic lncRNA in CRC.

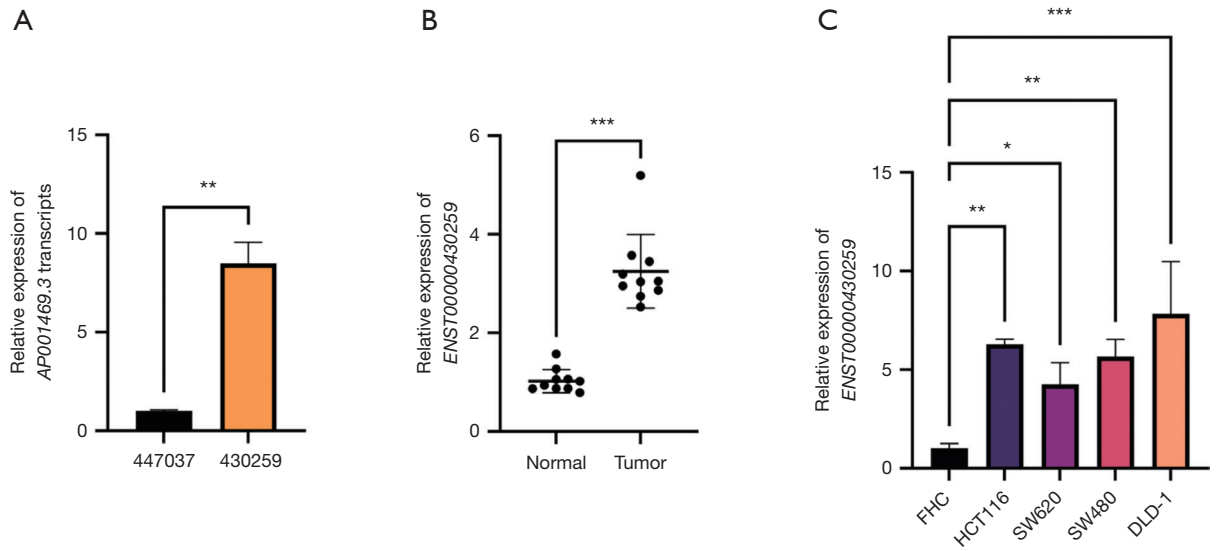

Figure 5 The transcript of *AP001469.3* gene *ENST00000430259* is overexpressed in CRC tissues and cell lines. (A) qRT-PCR showed that the expression level of transcript *ENST00000430259* in three cases of CRC tissues was much higher than that of transcript *ENST00000447037*. (B) qRT-PCR showed that *ENST00000430259* was aberrantly overexpressed in ten cases of CRC tissues when compared with their respective controls. (C) qRT-PCR showed that *ENST00000430259* expression was significantly higher in CRC cell lines (HCT116, SW620, SW480 and DLD-1) than in the normal intestinal epithelial cell line FHC. *, P<0.05; **, P<0.01; ***, P<0.001. CRC, colorectal cancer; qRT-PCR, quantitative real-time polymerase chain reaction; 447037, *ENST00000447037*; 430259, *ENST00000430259*.

GSEA of AP001469.3 gene in CRC

Subsequently, to better understand the differences in function, GSEA was performed in CRC to explore the main biological process affected by *AP001469.3*. KEGG-related GSEA revealed that the top five signaling pathways including cell adhesion molecules (CAMs), graft versus host disease, hematopoietic cell lineage, intestinal immune network for IgA production and Leishmania infection were all significantly enriched in the low-*AP001469.3* expression group (*Figure 7A*). Moreover, GO-related GSEA revealed that the top five signaling pathways including humoral immune response mediated by circulating immunoglobulin, immunoglobulin complex, immunoglobulin complex circulating, antigen binding and immunoglobulin receptor binding were all significantly enriched in the low-*AP001469.3* expression group (*Figure 7B*). The results showed that *AP001469.3* might regulate the biological process of CRC mainly through the above pathways.

Discussion

CRC is one of the most common gastrointestinal tumors with poor prognosis. It has become the second leading cause of cancer-related mortality worldwide (1). Despite the research progress of CRC treatment, however, the molecular mechanisms and biological processes of CRC still remain to be clarified. Thus, finding key genes and understanding their functions in regulating CRC occurrence and development are essential to effectively treating CRC. On the other hand, lncRNAs have been shown to modulate cancer progression by influencing the molecular characteristics of tumors, such as tumor microenvironment (8,24). For example, lncRNA MIR17HG was confirmed to regulate TIME and play an oncogenic role in CRC (25). In this study, we investigated the expression level of *AP001469.3* gene in pan-cancer including CRC and explored its association with clinical pathological characteristics in CRC using TCGA RNA-seq data. The relationships between *AP001469.3* expression and TIME, including StromalScore, ImmuneScore, ESTIMATEScore, TMB, MSI, ICI, ICP genes and IPS, were analyzed subsequently. Then, *in vitro* experiments were performed to explore the effects of *AP001469.3* on the biological behavior of CRC cells. We also performed GSEA to find the potential signaling pathways by which *AP001469.3* regulated CRC progression.

AP001469.3 is a lncRNA gene located on chromosome

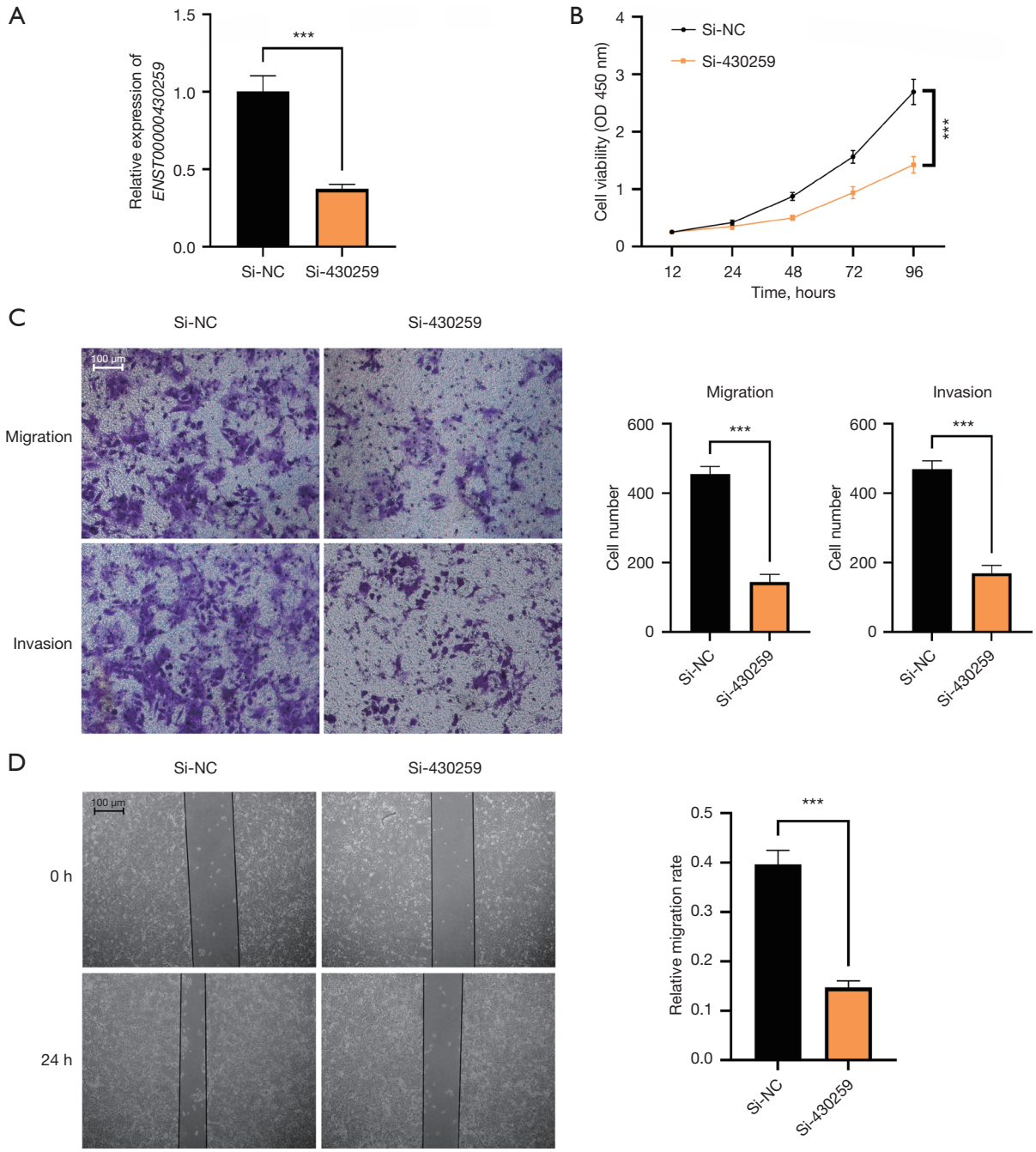

Figure 6 *ENST00000430259* functions as an oncogenic lncRNA *in vitro* in CRC. (A) *ENST00000430259* was knocked down in DLD-1 cells by transfecting siRNA targeting *ENST00000430259*, and the efficiency of knockdown was verified by qRT-PCR. (B) CCK-8 assays revealed that *ENST00000430259* knockdown suppressed the proliferation of DLD-1 cells. (C) Transwell assays revealed that *ENST00000430259* knockdown reduced the migration and invasion abilities of DLD-1 cells. Scale bars: 100 μm. Staining method: crystal violet staining. (D) Wound healing assays showed that *ENST00000430259* knockdown reduced the migration abilities of DLD-1 cells. Scale bars: 100 μm. Observation method: the scratch areas were photographed under a ×40 phase contrast microscope at 0 and 24 h. Relative migration rate was calculated as the follows: (original scratch width-scratch width at 24 h)/(original scratch width). ***, P<0.001. lncRNA, long non-coding RNA; CRC, colorectal cancer; siRNA, small interfering RNA; qRT-PCR, quantitative real-time polymerase chain reaction; CCK-8, cell counting kit-8; Si, small interfering; NC, negative control; 430259, *ENST00000430259*; OD, optical density.

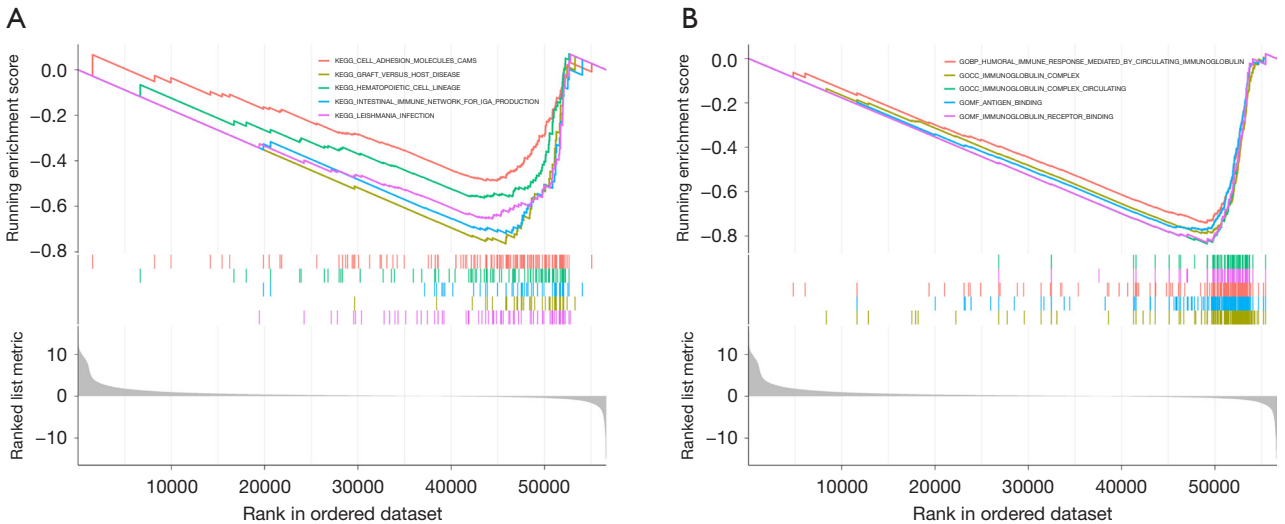

Figure 7 GSEA of *AP001469.3* gene in CRC. (A) The top five differentially enriched KEGG pathways between the high- and low-*AP001469.3* expression groups with the GSEA analysis. (B) The top five differentially enriched GO pathways between the high- and low-*AP001469.3* expression groups with the GSEA analysis. The peak of the upward and downward curve indicates the positive and negative regulation of *AP001469.3*, respectively. GSEA, gene set enrichment analysis; CRC, colorectal cancer; KEGG, Kyoto Encyclopedia of Genes and Genomes; GO, Gene Ontology; BP, biological process; CC, cellular component; MF, molecular function.

21: 46,251,549-46,254,133 reverse strand and its Ensembl ID is *ENSG00000239415* (23,26). Recently, *AP001469.3* was reported by Chen *et al.* (27) to participate in the construction of a ferroptosis-related lncRNA model, which showed promising clinical predictive value for CRC patients. In addition, Lin *et al.* (28) also established a novel ferroptosis-related lncRNA prognostic signature in hepatocellular carcinoma, which included *AP001469.3*. Using TCGA and ImmPort databases and bioinformatics methods, Sun *et al.* (13) screened the immune-related lncRNA gene *AP001469.3* and found it was differentially expressed between CRC tissues and normal tissues. Our results demonstrated that the expression of *AP001469.3* was up-regulated in CRC, and high expression of *AP001469.3* was associated with a higher M stage and a higher TNM stage in CRC, which suggested that *AP001469.3* possibly play a critical role in the malignant progression of CRC. Consistently, the KM survival analysis showed that CRC patients in the high-*AP001469.3* expression group had significantly shorter OS time than those in the low-*AP001469.3* expression group when choosing the optimal cut-off value, indicating that high-*AP001469.3* expression would predict a worse survival outcome.

Then, our ESTIMATE analysis showed that the low-*AP001469.3* expression group had higher StromalScore, ImmuneScore and ESTIMATEScore than the high-*AP001469.3* expression group, suggesting that *AP001469.3* might participate in regulating the TIME of CRC. To better explore the role of *AP001469.3* in the TIME of CRC, the correlations between *AP001469.3* expression and ICI levels and ICP genes expression were analyzed. In CRC samples, *AP001469.3* expression was significantly and positively correlated with the infiltration levels of monocytes, resting memory CD4 T cells and activated NK cells, but significantly and negatively correlated with the infiltration levels of M2 macrophages and neutrophils. In addition, the majority of the ICP genes were significantly and negatively correlated with *AP001469.3* expression in CRC. As known, immune response to cancer cells is a crucial factor in determining cancer prognosis, and immune cells such as lymphocytes, macrophages, granulocytes, dendritic cells and mast cells play a key role in determining the effects of anti-cancer immunotherapy (29-32). Researches also have proven that ICP genes play important roles in recruiting immune cells and reconstructing the immune microenvironment (17). Moreover, upregulation of ICP genes was positively correlated with high immune activity, good prognosis and better immunotherapy response (33). In order to assess the value of *AP001469.3* in the prediction of immunotherapy response in CRC, we analyzed the IPS scores of different *AP001469.3* expression groups in CRC patients based on the TCIA database, and found that the

IPS scores of low-*AP001469.3* expression group were higher than those of high-*AP001469.3* expression group in subgroups of CTLA-4 negative PD-1 positive and CTLA-4 positive PD-1 positive. Evidence presented that a higher IPS for a patient indicates that the patient can benefit from immunotherapy (22), and therefore our results indicated that CRC patients with low-*AP001469.3* expression could benefit much from immunotherapy based on anti-PD-1. In addition, CRC patients with high microsatellite instability/deficient mismatch repair (MSI-H/dMMR) tumors have been confirmed to be more responsive to immunotherapy (26,27), which was consistent with our correlation analysis result that *AP001469.3* was significantly and negatively correlated with MSI in COAD. Consequently, we speculated that *AP001469.3* could be potentially used as an immunotherapeutic indicator for CRC.

Using the Ensembl database, we found that *AP001469.3* gene has two transcripts *ENST00000447037* and *ENST00000430259* (23). Then we found that in CRC tissues, the expression abundance of transcript *ENST00000430259* was substantially higher than that of transcript *ENST00000447037*, indicating that *ENST00000430259* might play a leading role in the biological function of *AP001469.3* gene. Our results showed that *ENST00000430259* was aberrantly overexpressed in CRC tissues and cell lines when compared with their respective controls. In our *in vitro* experiments, we subsequently investigated the role of *ENST00000430259* in the biological behavior of CRC cells. As shown in the results, knockdown of *ENST00000430259* suppressed the proliferation, migration and invasion of CRC cells, indicating that the transcript of *AP001469.3* gene *ENST00000430259* promoted the malignant progression of CRC. Finally, we explored the molecular functional mechanism of *AP001469.3* in CRC progression using GSEA. For example, CAMs pathway was the top differentially enriched KEGG pathway between the high- and low-*AP001469.3* expression groups, indicating that *AP001469.3* might exert its functions in CRC by regulating CAMs expression. As known, CAMs have been reported to mediate signals involved in tumor cell invasiveness, sustained proliferative capacity, and drug resistance both *in vitro* and *in vivo* (34). Intriguingly, our GSEA results also showed that the majority of the differentially enriched signaling pathways between the high- and low-*AP001469.3* expression groups were immune-related, indicating that *AP001469.3* might exert its biological functions in CRC mainly through immune-related pathways *in vivo*.

This study also had certain limitations. First, the results of our study were mainly based on the analysis of publicly available databases, and further basic experimental researches should be carried out. For example, *in vivo* experiments are needed to unveil the role of *AP001469.3*-mediated TIME in the regulation of CRC progression. Second, further clinical researches are needed to determine the role of *AP001469.3* expression in the prediction of immunotherapy response in CRC.

Conclusions

Taken all together, our study demonstrated that *AP001469.3* overexpression indeed promoted CRC progression and could predict a worse immunotherapy response in CRC patients. Therefore, *AP001469.3* may be a potential therapeutic target for CRC patients.

Acknowledgments

The authors sincerely thank all participants who participated in this study.
Funding: This work was supported by the National Natural Science Foundation of China (No. 81470881 to Z.F.); the Nanjing Medical University Science and Technology Development Foundation (No. NMUB2020339 to T.C.); and the Nanjing Pukou People's Hospital Science and Technology Development Foundation (No. KJ2022-22 to T.C.).

Footnote

Reporting Checklist: The authors have completed the MDAR reporting checklist. Available at https://tcr.amegroups.com/article/view/10.21037/tcr-24-145/rc

Data Sharing Statement: Available at https://tcr.amegroups.com/article/view/10.21037/tcr-24-145/dss
Peer Review File: Available at https://tcr.amegroups.com/article/view/10.21037/tcr-24-145/prf

Conflicts of Interest: All authors have completed the ICMJE uniform disclosure form (available at https://tcr.amegroups.com/article/view/10.21037/tcr-24-145/coif). The authors have no conflicts of interest to declare.

Ethical Statement: The authors are accountable for all aspects of the work in ensuring that questions related

to the accuracy or integrity of any part of the work are appropriately investigated and resolved. The study was conducted in accordance with the Declaration of Helsinki (as revised in 2013). The study was approved by the Ethics Committee of the First Affiliated Hospital of Nanjing Medical University, China (No. 2023-SR-206) and informed consent was obtained from all individual participants.

References

1. Sung H, Ferlay J, Siegel RL, et al. Global Cancer Statistics 2020: GLOBOCAN Estimates of Incidence and Mortality Worldwide for 36 Cancers in 185 Countries. CA Cancer J Clin 2021;71:209-49.
2. Shin AE, Giancotti FG, Rustgi AK. Metastatic colorectal cancer: mechanisms and emerging therapeutics. Trends Pharmacol Sci 2023;44:222-36.
3. Tian Y, Wang Y, Wen N, et al. Prognostic factors associated with early recurrence following liver resection for colorectal liver metastases: a systematic review and meta-analysis. BMC Cancer 2024;24:426.
4. Shebbo S, Binothman N, Darwaish M, et al. Redefining the battle against colorectal cancer: a comprehensive review of emerging immunotherapies and their clinical efficacy. Front Immunol 2024;15:1350208.
5. Al Zein M, Boukhdoud M, Shammaa H, et al. Immunotherapy and immunoevasion of colorectal cancer. Drug Discov Today 2023;28:103669.
6. Li S, Peng M, Tan S, et al. The roles and molecular mechanisms of non-coding RNA in cancer metabolic reprogramming. Cancer Cell Int 2024;24:37.
7. Wu S, Wu Y, Deng S, et al. Emerging roles of noncoding RNAs in human cancers. Discov Oncol 2023;14:128.
8. Zhang M, Wu Y, Mou J, et al. The global landscape of immune-derived lncRNA signature in colorectal cancer. Heliyon 2024;10:e25568.
9. Kumar D, Sahoo SS, Chauss D, et al. Non-coding RNAs in immunoregulation and autoimmunity: Technological advances and critical limitations. J Autoimmun 2023;134:102982.
10. Park EG, Pyo SJ, Cui Y, et al. Tumor immune microenvironment lncRNAs. Brief Bioinform 2022;23:bbab504.
11. Xiong Y, Wang Y, Tiruthani K. Tumor immune microenvironment and nano-immunotherapeutics in colorectal cancer. Nanomedicine 2019;21:102034.
12. Alzamami A. Implications of single-cell immune landscape of tumor microenvironment for the colorectal cancer diagnostics and therapy. Med Oncol 2023;40:352.
13. Sun M, Zhang T, Wang Y, et al. A Novel Signature Constructed by Immune-Related LncRNA Predicts the Immune Landscape of Colorectal Cancer. Front Genet 2021;12:695130.
14. Goldman MJ, Craft B, Hastie M, et al. Visualizing and interpreting cancer genomics data via the Xena platform. Nat Biotechnol 2020;38:675-8.
15. Yoshihara K, Shahmoradgoli M, Martínez E, et al. Inferring tumour purity and stromal and immune cell admixture from expression data. Nat Commun 2013;4:2612.
16. Newman AM, Liu CL, Green MR, et al. Robust enumeration of cell subsets from tissue expression profiles. Nat Methods 2015;12:453-7.
17. Topalian SL, Drake CG, Pardoll DM. Immune checkpoint blockade: a common denominator approach to cancer therapy. Cancer Cell 2015;27:450-61.
18. Liberzon A, Birger C, Thorvaldsdóttir H, et al. The Molecular Signatures Database (MSigDB) hallmark gene set collection. Cell Syst 2015;1:417-25.
19. Ros J, Baraibar I, Saoudi N, et al. Immunotherapy for Colorectal Cancer with High Microsatellite Instability: The Ongoing Search for Biomarkers. Cancers (Basel) 2023;15:4245.
20. Li DD, Tang YL, Wang X. Challenges and exploration for immunotherapies targeting cold colorectal cancer. World J Gastrointest Oncol 2023;15:55-68.
21. Sharma P, Goswami S, Raychaudhuri D, et al. Immune checkpoint therapy-current perspectives and future directions. Cell 2023;186:1652-69.
22. Charoentong P, Finotello F, Angelova M, et al. Pan-cancer Immunogenomic Analyses Reveal Genotype-Immunophenotype Relationships and Predictors of Response to Checkpoint Blockade. Cell Rep 2017;18:248-62.
23. Martin FJ, Amode MR, Aneja A, et al. Ensembl 2023. Nucleic Acids Res 2023;51:D933-41.

24. Shakhpazyan NK, Mikhaleva LM, Bedzhanyan AL, et al. Long Non-Coding RNAs in Colorectal Cancer: Navigating the Intersections of Immunity, Intercellular Communication, and Therapeutic Potential. Biomedicines 2023;11:2411.
25. Xu J, Meng Q, Li X, et al. Long Noncoding RNA MIR17HG Promotes Colorectal Cancer Progression via miR-17-5p. Cancer Res 2019;79:4882-95.
26. Li Z, Cai S, Li H, et al. Developing a lncRNA Signature to Predict the Radiotherapy Response of Lower-Grade Gliomas Using Co-expression and ceRNA Network Analysis. Front Oncol 2021;11:622880.
27. Chen W, Deng J, Zhou Y. The construction of a novel ferroptosis-related lncRNA model to predict prognosis in colorectal cancer patients. Medicine (Baltimore) 2023;102:e33114.
28. Lin X, Yang S. A prognostic signature based on the expression profile of the ferroptosis-related long non-coding RNAs in hepatocellular carcinoma. Adv Clin Exp Med 2022;31:1099-109.
29. Park J, Hsueh PC, Li Z, et al. Microenvironment-driven metabolic adaptations guiding CD8(+) T cell anti-tumor immunity. Immunity 2023;56:32-42.
30. Laskowski TJ, Biederstädt A, Rezvani K. Natural killer cells in antitumour adoptive cell immunotherapy. Nat Rev Cancer 2022;22:557-75.
31. Kang BH, Lee HK. Dendritic Cell-Based Immunotherapy in Hot and Cold Tumors. Int J Mol Sci 2022;23:7325.
32. Oliveira G, Wu CJ. Dynamics and specificities of T cells in cancer immunotherapy. Nat Rev Cancer 2023;23:295-316.
33. Hu FF, Liu CJ, Liu LL, et al. Expression profile of immune checkpoint genes and their roles in predicting immunotherapy response. Brief Bioinform 2021;22:bbaa176.
34. Lin W, Fang J, Wei S, et al. Extracellular vesicle-cell adhesion molecules in tumours: biofunctions and clinical applications. Cell Commun Signal 2023;21:246.

Cite this article as: Chen T, Jiang Q, Wang Z, Zhang H, Fu Z. The roles of lncRNA *AP001469.3* in clinical implications, immune landscape and carcinogenesis of colorectal cancer. Transl Cancer Res 2024;13(7):3465-3481. doi: 10.21037/tcr-24-145

